Spatial Domain Decision Based Image Fusion Using Superimposition

Maitreyi Abhyankar, Arti Khaparde
Department of E&TC
Maharashtra Institute of Technology, SPPU
Pune, India
arti.khaparde@mitpune.edu.in
maitreyi_abhyankar@yahoo.com

Vaidehi Deshmukh
Department of E&TC
RMD College of Engineering, SPPU
Pune, India.
vaidehideshmukh@sinhgad.edu

Abstract— Image fusion is the process to combine two or more images such that the enhanced output image contains all the relevant information. This paper aims to evaluate algorithms that fuses multi-focus images. With an aim to enhance the sharpness of the final fused image and also to reduce the computational complexity, a novel method is proposed that uses the Sobel operator. This method is evaluated using mean squared error, peak signal to noise ratio, structural similarity index, entropy, mutual information, image quality index and run time. The optimum weights required to fuse two images are calculated from image statistics using genetic algorithm (GA). The results show that this superposition method performs at par with discrete wavelet transform (DWT) with reduction in run time.

Keywords—Image fusion, superimposed, Sobel operator, GA

I. INTRODUCTION

Image fusion forms a new image that is more informative than its constituent images. Due to non-uniform distance of objects from camera and limited depth-of-focus of the camera lens, not all the objects can be focused upon simultaneously. However, it is possible to obtain a number of images, each with a different object in focus, which can be combined together using image fusion techniques to get a final image with all the scene objects in focus [1].

The fusion of images can take place at two different levels-pixel based low level and decision based high level [2]. The pixel based techniques act upon the corresponding pixels of the input images. On the other hand, the decision based techniques take into account various features of the images such as edges or regions. These techniques have the advantage of lesser noise sensitivity and better contrast compared to the pixel based techniques, at the cost of complexity.

Image fusion techniques can also be broadly classified into two categories-spatial domain techniques and transform domain techniques [3]. Spatial domain methods directly work on the pixel value, whereas transform domain techniques include transforming the images using mathematical equations.

A simple spatial domain technique results in images that have poor contrast and sharpness. Another pixel level image fusion method involves giving the entire image as an input to the genetic search [7]. However, this method is computationally very expensive.

There are pyramid based methods, whose basic principle is to decompose the original image into pieces of sub-images with different spatial resolutions through some mathematical operations. The Laplacian pyramid is derived from the Gaussian pyramid, which is a multi-scale representation obtained through a recursive low-pass filtering and decimation. So, the Laplacian pyramid decomposition is divided into two steps: the first is Gaussian pyramid decomposition, the second is from Gaussian pyramid to Laplacian pyramid [5]. Thus such method uses the second order derivatives, which are more immune to noise.

However, the proposed novel technique used the first order derivative without decomposing the original image into sub-images with different spatial resolutions. Thus reducing the mathematical complexity. It uses two steps to fuse an image-firstly it finds the edges using edge detection method and then they are given as input to genetic algorithm for calculating the weights in which the two images should be fused.

The remainder of the paper is organised as follows: Section II describes the proposed algorithm. Section III gives the parameters on which the evaluation were done. Section IV deals with the results and Section V is conclusion..

II. PROPOSED METHOD

A. Superimposing Sobel detected edges

Focus and sharpness are features closely related to the quality of the image. Sharper images have more information than the blurred ones. It is often observed that fused images have blurred edges. Thus with an aim to improve the edge sharpness of the fused images, this algorithm superimposes the edges on the input images.

The Sobel operator uses different kernels to detect edges along x and y directions. The kernels are designed to respond maximally to the edges that are vertical and horizontal, relative to the pixel grid. The Sobel operator is a combination of differentiation and Gaussian smoothing, thus making it more resistant to noise, compared to the Prewitt operator. It not only gives an estimate of the direction of the edge, but also gives the

magnitude of the edge at a particular point. Canny edge detector requires careful selection of the two thresholds without which the edges are not detected properly. Thus Sobel operator was chosen to give good results avoiding the critical selection of the threshold values.

The algorithm proceeds by detecting the edges for the input images. The kernel used to detect edges along x direction is:

$$\begin{bmatrix} -1 & 0 & 1 \\ -2 & 0 & 2 \\ -1 & 0 & 1 \end{bmatrix} \quad (1)$$

The edges along y direction are detected using:

$$\begin{bmatrix} -1 & -2 & -1 \\ 0 & 0 & 0 \\ 1 & 2 & 1 \end{bmatrix} \quad (2)$$

The edges are then averaged to form a new edge image E. This image is superimposed on the first input using weighted addition method.

$$Image3 = k1*Image1 + k2*E \quad (3)$$

$$k_1 = \frac{Avg\ pixel\ value\ in\ Image_1}{Max\ pixel\ value\ in\ Image_1} \quad (4)$$

$$k_2 = (1 - k_1)*0.1 \quad (5)$$

The intermediate image Image3 is superimposed on the second input image to form the final output image.

$$Final = k_3 * Image_2 + k_4 * Image_3 \quad (6)$$

$$k_3 = 1 - \left(\frac{Average\ pixel\ value\ in\ Image_2}{Max\ pixel\ value\ in\ Image_2} \right) \quad (7)$$

$k_4 = 1$ (as it is used for the intermediate image that is already superimposed) $\quad (8)$

B. Feature vector for Sobel based GA

For Sobel based genetic algorithm, the Sobel operator is applied along x and y directions forming two edge images. Normalised central moments up to order 3 for each edge image are calculated-forming a total of 16 moments. Mean and standard deviation of edges along x and y directions are calculated. Finally, the feature vector of size 1 X 20 is formed by combining the moments, mean and standard deviation.

C. Genetic algorithm based on edges detected by Sobel operator

The genetic search [7] implemented starts by generating a population of size 100. This population consists of randomly generated binary strings of length 10. Before evaluating the individuals, they are converted from binary to decimal equivalent such that every binary string lies in the range of 0 to This conversion is given as:

$$L_l + (U_l - L_l) * Decimal\ equivalent\ /\ (2^n - 1) \quad (9)$$

Where, Lower limit (L_l)=0, Upper limit (U_l) =1, n = Number of bits in the binary.

The individuals are evaluated using mean squared error as the fitness function. Mathematically, this fitness function is given as:

Fitness=

$$\left\{ \frac{1}{2} \left(\frac{1}{d} \sum_{i=1}^{d} [F_{int}(i) - Img_1(i)]^2 \right) + \left(\frac{1}{d} \sum_{i=1}^{d} [F_{int}(i) - Img_2(i)]^2 \right) \right\} \quad (10)$$

d is the dimension of the input vector which is 1 x 40, calculated as described in section II B. $F_{int}(i)$ is the intermediate fused image obtained by using the equation:

$$F_{int}(i) = W_{int1} * Img_1 + W_{int2} * Img_2 \quad (11)$$

Img_1 and Img_2 are the input images, W_{int1} is the weight individual being evaluated and:

$$W_{int2} = (1 - W_{int1}) \quad (12)$$

The value of this fitness function should be as small as possible. However, it can also be transformed to make this fitness function a maximisation fitness using the function:

$$F(x) = 1/(1 + Fitness) \quad (13)$$

Selection is done by considering the individuals that have the highest fitness values. Different methods exist for the selection process such as- Roulette wheel selection, Rank based selection, Tournament selection etc. [7] uses tournament based selection method with a tournament size of 2. The next step is performing crossover and mutation operations on the selected individuals. It uses a crossover probability of 0.7 and a mutation probability of 0.002. Uniform crossover and bit-flip mutation is used. These modified individuals replace the existing population. The process is repeated for 25 generations. It is experimentally observed that this search is converging in 20-23 generations. After the last generation, the optimum candidate is selected. The second weight is obtained as (1-W_1). On obtaining the two weights, each is assigned to the input images. Final fused image is obtained as a result of the addition of these optimally weighted images as:

$$F_{final} = W_1 * Img_1 + W_2 * Img_2 \quad (14)$$

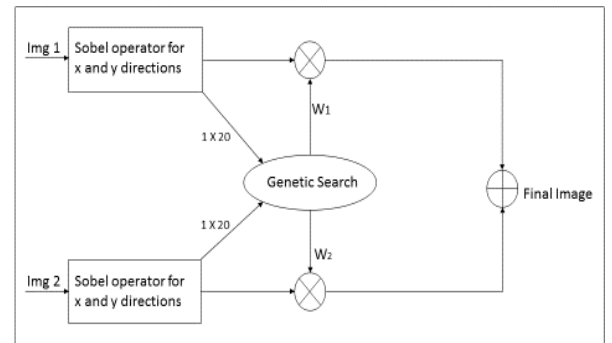The block diagram for the process is described in Figure 1:

Fig. 1 Flow Diagram for Proposed method

III. EVALUATION OF THE FUSED IMAGES:

The basic requirement is that the output images should contain all the valid and useful information present in the source images without introducing any form of distortion. The resultant images can be compared visually, but, these methods, though

very powerful, are subjective in nature. Hence, objective statistical methods are used [1-9].

1) Root Mean Squared Error:

$$\text{RMSE} = \sqrt[2]{\frac{1}{mn} \left[\sum_{i=0}^{m-1} \sum_{j=0}^{j-1} Img1(i,j) - Img2(i,j)\right]^2} \tag{15}$$

m, n: size of the input images Img1 and Img2

2) Peak Signal to Noise Ratio:

Peak signal to noise ratio gives the ratio of the maximum power of a signal and the power of corrupting noise.

$$\text{PSNR} = 20 \log 10 \left(\frac{Max}{\sqrt{MSE}}\right) \tag{16}$$

Max: Maximum possible pixel value, as 8 bits are used to represent a pixel, Max=255

3) Structural similarity index:

$$\text{SSIM (x, y)} = \frac{(2\mu_x\mu_y + c_1)(2\sigma_{xy} + c_2)}{(\mu_x^2 + \mu_y^2 + c_1)(\sigma_x^2 + \sigma_y^2 + c_2)} \tag{17}$$

Where μ_x the average of x; μ_y the average of y;

σ_x^2 the variance of x; σ_y^2 the variance of y;

σ_{xy} the covariance of x and y;

$$c1 = (k_1 L)^2, \; c2 = (k_2 L)^2 \tag{18}$$

L is the dynamic range of the pixel-values; $k_1 = 0.01$ and $k_2 = 0.03$ by default.

SSIM is used to model any image distortion as a combination of correlation losses, radiometric and contrast distortions. Higher the value of SSIM, more similar are the images. It can have a maximum possible value of 1.

4) Entropy:

Entropy is used to give the amount of information contained in an image. Mathematically it is given as:

$$\text{E} = -\sum_{i=0}^{L-1} P_i log_2 P_i \tag{19}$$

P_i is the probability of occurrence of a pixel value in the image, L is the number of intensity levels in the image. Increase in the value of entropy after fusion indicates that the information contained in the image has increased.

5) Mutual Information:

It is an indicator of the information obtained from the source images and the quantity that is conveyed by the fused image.

$$\text{MI} = MI_{F,I1} + MI_{F,I2} \tag{20}$$

$$MI_{F,I1} = \sum P_{F,I1}(f, i1) \log_2 \frac{P_{F,I1}(f,i1)}{P_F(f) P_{I1}(i1)} \tag{21}$$

$$MI_{F,I2} = \sum P_{F,I2}(f, i2) \log_2 \frac{P_{F,I2}(f,i2)}{P_F(f) P_{I1}(i2)} \tag{22}$$

Where $MI_{F,I1}$ denotes the mutual information between the fused image and the first input image, $MI_{F,I2}$ denotes the mutual information between the second input and the fused image, $P_{F,I1}(f,i1)$ and $P_{F,I2}(f,i2)$ are the joint histograms of fused image, input 1and fused image, input 2 respectively, $P_F(f), P_{I1}(i1)$ and $P_{I1}(i2)$ are the histograms of the fused image, input 1 and input 2 respectively.

6) Run Time:

It gives a measure of the time required for complete run of the algorithm in seconds.

7) Image Quality Index [9]:

Mathematically given as: $\frac{4\sigma_{xy}\bar{x}\bar{y}}{(\sigma_x^2 + \sigma_y^2)[(\bar{x})^2 + (\bar{y})^2]}$ (23)

where $\bar{x}, \bar{y}$ are the means of x and y respectively, σ_{xy} is the covariance of x and y, σ_x^2, σ_y^2 are the variances of x and y respectively.

IV. RESULTS

The algorithms : - Image Fusion Using Genetic Algorithm and Discrete Wavelet Transform proposed [6] and Genetic algorithm based on edges detected by Sobel operator were both implemented and tested on different types of images from a database of multi-focus images and also on real time images captured by a camera, focusing on different object in every image. The analysis of the result were done on the different parameters as explained in the pervious section. Here results for 6 images in each categoryy are shown for reference. For subjective analysis 50 subjects were considered. The subjective and objective analysis for the image from the database and for real time image caputered from camera is given in the Section IV. A and IV.B respectively.

A. Results for database image
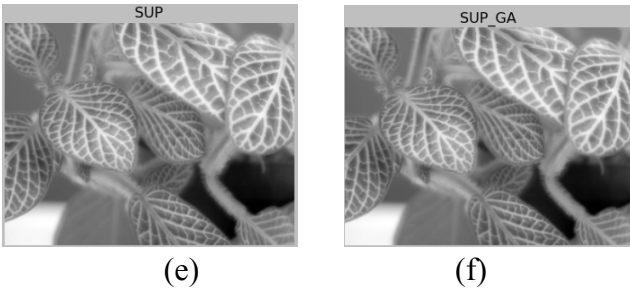

(a)   (b)

(c)   (d)

(e)   (f)
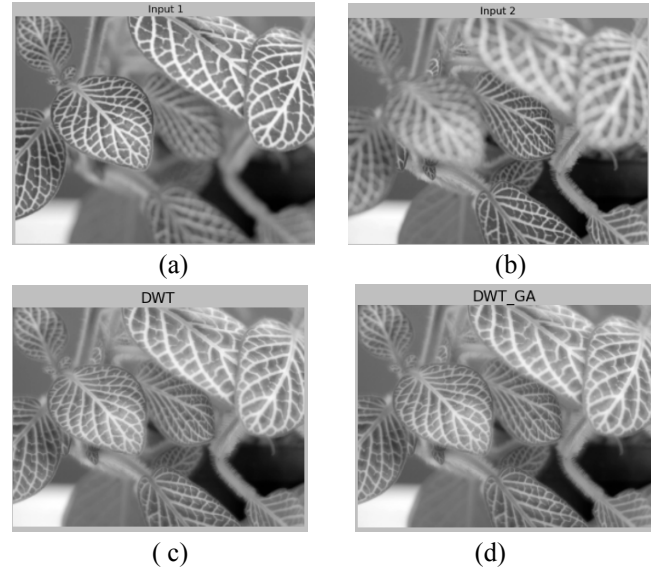
Fig. 2 (a)-(b): Data base input images, (c) DWT (d)DWT_GA (e) SUP (f) SUP_GA

TABLE I. COMPARISION RESULTS FOR DATABASE IMAGESET 1

Method Parameter	DWT	DWT_GA	SUP	SUP-GA
RMSE	12.29337633	12.29198814	12.46290628	12.29198814
PSNR	26.33740597	26.33934677	26.23599944	26.33934677
SSIM	0.813867487	0.813732134	0.81200342	0.813697015
ENTROPY	7.231954748	7.233046212	7.20405317	7.230991011
MI	4.517193245	4.542809862	4.520682512	4.541790674
IQI	0.789147424	0.788287993	0.781242432	0.788084485
TIME	0.107461748	0.774208658	0.005526063	0.641027041

TABLE II. (A)-(F) OBJECTIVE ANALYSIS OF DATABASE IMAGES

TABLE II. (A)

DB_ENTROPY			
	DWT	DWT_GA	SUP	SUP-GA
Img 1	7.274102079	7.276063705	7.279682645	7.276063705
Img 2	7.124278087	7.122863208	7.125016254	7.122863208
Img 3	7.401747586	7.402183644	7.436018162	7.401685456
Img 4	7.2651839	7.26871736	7.280613934	7.26871736
Img 5	7.630098537	7.62981082	7.633059902	7.62981082
Img 6	7.456101171	7.455349685	7.472908158	7.457472519

TABLE II. (B)

DB_RMSE			
	DWT	DWT_GA	SUP	SUP-GA
Img 1	1.91826451	1.91152555	1.94137463	1.91152555
Img 2	5.85085359	5.84905470	5.875658161	5.84905470
Img 3	4.22200801	4.21939606	5.378821475	4.21939606
Img 4	5.47229690	5.470035809	5.537205451	5.47003580
Img 5	8.22364723	8.221683078	8.279220459	8.2216830
Img 6	6.19894491	6.196928392	6.396782339	6.19692839

TABLE II. (C)

TABLE II. (D)

DB_PSNR			
	DWT	DWT_GA	SUP	SUP-GA
Img 1	42.472634	42.533424	42.477594	42.53342446
Img 2	32.786419	32.791667	33.25994	32.79166767
Img 3	35.620422	35.631023	33.517562	35.63102308
Img 4	33.367410	33.374527	33.293689	33.37452747
Img 5	29.829514	29.833611	29.826373	29.83361158
Img 6	32.284448	32.290016	32.018395	32.29001684

TABLE II. (E)

DB_SSIM			
	DWT	DWT_GA	SUP	SUP-GA
Img 1	0.982777041	0.982123634	0.981018979	0.982123634
Img 2	0.930889259	0.930452878	0.924458696	0.930452878
Img 3	0.956972799	0.956376947	0.955409133	0.956554622
Img 4	0.930143237	0.929757413	0.92827984	0.929798738
Img 5	0.87890549	0.87866285	0.876113805	0.878824499
Img 6	0.938319003	0.938011691	0.93627495	0.937855107

TABLE II. (E)

DB_MI			
	DWT	DWT_GA	SUP	SUP-GA
Img 1	9.551883011	9.655036852	9.567111012	9.655036852
Img 2	6.4997739	6.561308933	6.686758519	6.561451091
Img 3	7.827594187	7.905515019	7.814607012	7.905515019
Img 4	6.555595817	6.614265014	6.564783308	6.614265014
Img 5	5.574346778	5.60367631	5.602074868	5.60367631
Img 6	6.881332977	6.93498181	6.872462701	6.934162586

TABLE II. (F)

DB_IQI			
	DWT	DWT_GA	SUP	SUP-GA
Img 1	0.935682543	0.925304617	0.919558285	0.929710395
Img 2	0.873712795	0.87268237	0.861826782	0.87268237
Img 3	0.922875608	0.920257882	0.917886311	0.920339326
Img 4	0.900840182	0.898281339	0.896783403	0.898281339
Img 5	0.851772361	0.851094892	0.848525631	0.851094892
Img 6	0.876924905	0.876336084	0.873263578	0.873728318

Fig. 3 Comparison graph of run-time for database image sets

TIME	0.292187607	0.978869865	0.031723194	0.700341361

TABLE IV (A)-(F) OBJECTIVE ANALYSIS OF REAL TIME IMAGES
TABLE IV (A)

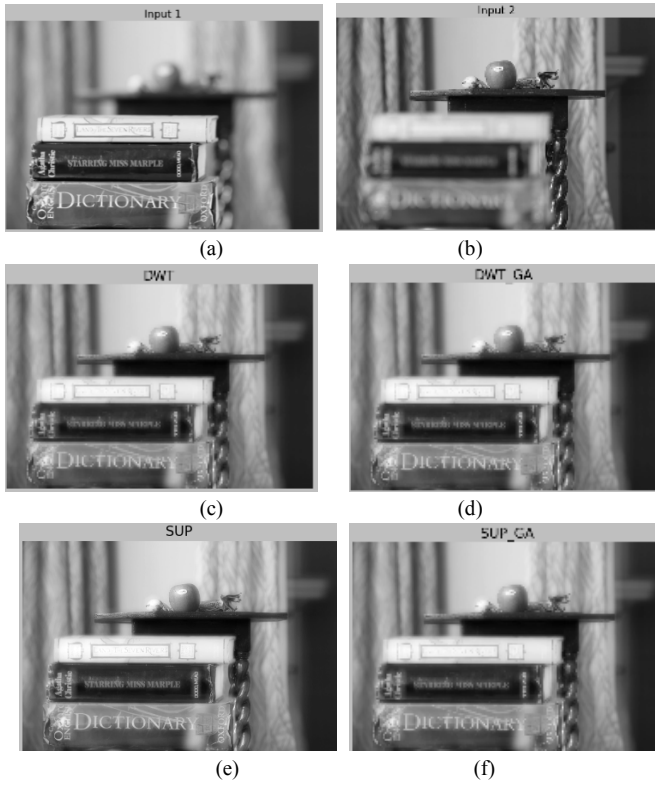| RT_ENTROPY				
	DWT	**DWT_GA**	**SUP**	**SUP-GA**
Img 1	7.579773661	7.580852115	7.498521817	7.58085211
Img 2	7.362242686	7.362771531	7.480970609	7.36169769
Img 3	7.261306599	7.261494279	7.243778203	7.26149427
Img 4	7.391961954	7.39242764	7.244967577	7.39177275
Img 5	7.438890956	7.439064454	7.212666618	7.43864487
Img 6	6.984488975	6.98400513	6.890249163	6.98400513

B. Results for real time images dataset

Figure 4: (a)-(b)In-house input images, (c)DWT, (d)DWT_GA, (e)SUP, (f)SUP_GA

TABLE III. COMPARISION RESULTS FOR REAL TIME IMAGE SET

Method Parameter	DWT	DWT_GA	SUP	SUP-GA
RMSE	16.34494177	16.34435492	18.35665383	16.34435492
PSNR	23.86342597	23.86403993	23.05998683	23.86403993
SSIM	0.842798432	0.842749184	0.839463641	0.842705444
ENTROPY	7.640887795	7.641077463	7.731927953	7.641090614
MI	5.301427461	5.30847386	5.332867629	5.308912345
IQI	0.653848904	0.653172121	0.647788754	0.653768346

TABLE IV (B)

RT_RMSE				
	DWT	**DWT_GA**	**SUP**	**SUP-GA**
Img 1	20.6532295	20.65286544	21.42743903	20.65286544
Img 2	16.65166062	16.65131342	19.13375733	16.65131342
Img 3	15.28754074	15.28654024	15.30659951	15.28654024
Img 4	28.56503167	28.56498326	29.53373719	28.56498326
Img 5	32.20576404	32.20574529	34.09786658	32.20574529
Img 6	27.04314846	27.04312433	28.15428863	27.04312433

TABLE IV (C)

RT_PSNR				
	DWT	**DWT_GA**	**SUP**	**SUP-GA**
Img 1	21.83124518	21.83154276	21.59659871	21.83154276
Img 2	23.70207574	23.70242563	22.57267635	23.70242563
Img 3	24.44412938	24.44525625	24.4737668	24.44525625
Img 4	19.01434398	19.01436827	18.85130113	19.01436827
Img 5	17.97233335	17.97233793	17.94376017	17.97331237
Img 6	19.48992689	19.48993356	19.16702031	19.48993356

TABLE IV (D)

RT_SSIM				
	DWT	**DWT_GA**	**SUP**	**SUP-GA**
Img 1	0.818907818	0.818984598	0.816233943	0.818984598
Img 2	0.849284887	0.849310637	0.844615324	0.849097836
Img 3	0.785957966	0.785965178	0.784197483	0.785965178
Img 4	0.762326912	0.762082945	0.760206148	0.762299459
Img 5	0.800947268	0.800945828	0.795289886	0.800945828
Img 6	0.821950081	0.821952094	0.816359774	0.821343789

TABLE IV (E)

RT_MI				
	DWT	**DWT_GA**	**SUP**	**SUP-GA**
Img 1	4.873001463	4.876984936	4.845757594	4.880716815

Img 2	5.394087435	5.398524661	5.481756653	5.398524661
Img 3	3.916171705	3.926452532	3.929623337	3.925354233
Img 4	5.002863171	5.004713836	5.212359849	5.006628048
Img 5	5.972325141	5.974694824	6.14354577	5.973201084
Img 6	5.969264311	5.969632032	6.565425717	5.969632032

TABLE IV (F)

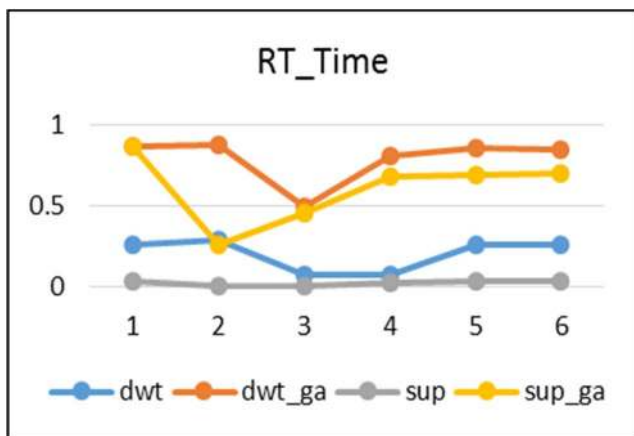| RT_IQI				
	DWT	**DWT_GA**	**SUP**	**SUP-GA**
Img 1	0.652062571	0.651698257	0.630641019	0.65211363
Img 2	0.658369523	0.658316622	0.647341452	0.65876612
Img 3	0.60742846	0.607292029	0.597639524	0.60693498
Img 4	0.555591296	0.555872199	0.51193606	0.55587219
Img 5	0.557462	0.558336755	0.510557324	0.55833675
Img 6	0.571653167	0.572877653	0.528519749	0.57169156

Fig. 5 Comparison graph of run time for real time image sets

V. CONCLUSION

The results obtained from the proposed method are similar to the results obtained from discrete wavelet transform and genetic algorithm based on DWT with respect to RMSE, PSNR and SSIM. The added advantage of the proposed method is its simplicity leading to lower run time compared to DWT and DWT based GA. It was also observed the most of the test images produced better entropy and mutual information values for the proposed method. Also the image quality index is slightly greater for the proposed method than DWT based GA in most of the tests. Subjective analysis shows that the contrast of the images fused by the proposed method have to be further improved. Thus algorithm can be further extended to fuse real time images in a quick and efficient manner which can be used in variety of applications.

REFERENCES

[1] Wei-We1 Wang, Peng-Lang Shui, Guo-Xiang Song,"Multifocus Image Fusion In Wavelet Domain", Proceedings of the Second International Conference on Machine Learning and Cybernetics, November 2003

[2] Tanish Zaveri, Mukesh Zaveri," A Novel Region based Image Fusion Method using High-boost Filtering", Proceedings of the 2009 IEEE International Conference on Systems, Man and Cybernetics, San Antonio, TX, USA, October 2009

[3] Yong Yang, Song Tong, Shuying Huang, Pan Lin, "Multi-focus Image Fusion Based on NSCT and Focused Area Detection", IEEE Sensors Journal, Vol. 15, No. 5, May 2015

[4] Hugo R. Albuquerque, Tsang Ing Ren, George D. C. Cavalcanti,"Image Fusion Combining Frequency Domain Techniques Based on Focus", IEEE 24th International Conference on Tools with Artificial Intelligence, 2012.

[5] Wencheng Wang, Faliang Chang, "A Multi-focus Image Fusion Method Based on Laplacian Pyramid", Journal Of Computers, Vol. 6, No. 12, December 2011, pp. 2559-2566

[6] Anjali Malviya, S. G. Bhirud, "Wavelet Based Multi-Focus Image Fusion", International Conference on Methods and Models in Computer Science, 2009

[7] Chaunté W. Lacewell, Mohamed Gebril, Ruben Buaba, Abdollah Homaifar, "Optimization of Image Fusion Using Genetic Algorithms and Discrete Wavelet Transform", Radar Signal & Image Processing, IEEE, 2010

[8] Yifeng Niu, Lincheng Shen, Lizhen Wu and Yanlong Bu," Optimizing the Number of Decomposition Levels for Wavelet-Based Multifocus Image Fusion", Proceedings of the 8th World Congress on Intelligent Control and Automation, Jinan, China, July 2010

[9] Zhou Wang, Alan C. Bovik, "A Universal Image Quality Index", IEEE Signal Processing Letters, March 2002.